

Coil in Coil – Components for the High Voltage Superconducting Resistive Current Limiter CULT 110

Steffen Elschner⁽²⁾, Mark Stemmler⁽³⁾, Frank Breuer⁽¹⁾, Heribert Walter⁽¹⁾, Christian Frohne⁽³⁾, Mathias Noe⁽⁴⁾ and Joachim Bock⁽¹⁾

(1) Nexans SuperConductors GmbH, D 50351 Huerth, Germany

(2) Hochschule Mannheim, D 68163 Mannheim, Germany

(3) Nexans Deutschland Industries GmbH & Co. KG, D 30179 Hannover, Germany

(4) Forschungszentrum Karlsruhe GmbH, D 76021 Karlsruhe, Germany

E-Mail: mark.stemmler@nexans.com

Abstract - The project CULT 110 funded by German government (BMBF/VDI) is presently the largest current limiter project in Europe. It aims at the development of a one-phase resistive limiter for the 110 kV level and is based on melt cast processed BSCCO 2212 bulk superconductor. The innovative electrical protection concept uses a normal conducting coil arranged around the superconducting bulk coil and connected in parallel. This coil serves as an electrical bypass and simultaneously, under fault conditions, generates a magnetic field for quench homogenisation. Since no continuously connected shunt is needed, an increased voltage can be applied during faults.

Manuscript received December 14, 2007; accepted Jan 11, 2008. Reference No. ST24, Category 6. Based on paper submitted to Proceedings of EUCAS 2007; published in JPCS 98 (2008), paper # 012309

I. INTRODUCTION

Fault current limiters are at present one of the most attractive applications of high-temperature superconductors in electric power systems [1]. Especially resistive concepts [2-5] seem to have excellent chances for economical and technical viability. This was shown, up to the 10 kV/10 MVA rating, *e.g.*, within the successful German current limiter project CURL 10 [3], which utilized melt cast processed (MCP) BSCCO 2212 as the superconductor.

On the basis of CURL 10 achievements, the German government (BMBF/VDI) funded the new project CULT 110 which started in 2005. It aims at the construction of a 1-phase superconducting resistive fault current limiter demonstrator for the 110 kV grid. The consortium gathers together partners with all the necessary skills for such a complex project. The German utility RWE defined a set of specifications and is committed to test in the future a full-scale 3-

phase prototype in grid operation, after the successful development of a single phase demonstrator. Forschungszentrum Karlsruhe (ITP) is responsible for the high voltage design, Leibniz University Hannover supports the project partners with simulations, Nexans Deutschland Industries establishes the cryogenic concept and Nexans SuperConductors develops the components and assembles the whole system.

The technical specifications to be met by the 1-phase-demonstrator are based on the requirements for the 3-phase prototype intended to be installed in a grid coupling [6] between two RWE 110 kV grids. Main technical challenges are the rated current $I_r = 1850$ A and the limitation time $t_{lim} = 60$ ms. The prospective short circuit current of 31.5 kA (peak current 80 kA) must be limited to 6 kA with the first peak not exceeding 40 kA.

An important task of all resistive fault current limiter projects is a reliable protection concept against the dangers of hot spots. The concept used successfully within CURL 10 [3], a normal-conducting bypass soldered continuously on the superconductor, is not transferable to the high-voltage level. Due to the heating of the shunt, the voltage in the limitation case must not exceed 1 V/cm leading to prohibitively long lengths. Therefore, a novel protection concept has been proposed [4,7], which is based on the strong magnetic field dependence of critical current density. Indeed, at 77 K the critical current density decreases by one order of magnitude in a field as small as 0.1 T [7]. The new concept consists of a normal-conducting coil arranged around the bulk superconductor and connected in parallel (Figure 1). If a short circuit occurs, a voltage along the superconductor appears due to flux flow and/or the formation of hot spots. This voltage drives a current through the normal conducting coil. The resulting field then brings the still superconducting parts of the sample to a fast and homogeneous quench.



Fig 1. Coil-in-coil component. The superconducting coil machined out of a tube (inner) is introduced into the normal-conducting trigger coil (outer) and connected in parallel.

This contribution describes the design rules for suitable components, *i.e.* the superconducting coils and normal-conducting trigger coils. We show by simulation and experiment, that the proposed protection mechanism works reliably.

II. SUPERCONDUCTING COILS

Initially, the new protection mechanism was proposed for tube-shaped superconductors with normal-conducting trigger coils [4, 7]. However this concept has quite large losses under normal operating conditions: With a rated current of 1850 A, an effective tube length of 30 cm and an assumed resistance of 1 $\mu\Omega$ per component (copper plus 2 contacts), normal conducting losses of about 3 kW per phase at 77 K are expected. These losses can be reduced considerably if we use coils machined out of superconducting tubes. For the set tube diameter, the superconducting length of each coil significantly exceeds the length of the tube. Consequently, a lesser number of components is required in the string ($m' < m$). However, to attain the required current rating (the superconductor cross-section), several such strings must be connected in parallel to form an array. The number k of parallel strings increases with decreasing coil pitch, in our case $k \approx 10$. As the product of superconducting length and total cross-section must be constant, the volume of superconducting material and consequently the total number of components remains roughly unchanged when compared with the tube-in-coil design, $m = km'$. The current in each component is reduced by the factor k and thus the total losses in the contacts decrease by a factor k^2 . Figure 2 depicts schematically both the old tube-in-coil design (a), and the new coil-in-coil-design (b).

A further advantage of the coil-in-coil design is that the trigger field and self field have the same direction and their values add up directly, whereas in the tube-in-coil design both fields are perpendicular to each other.

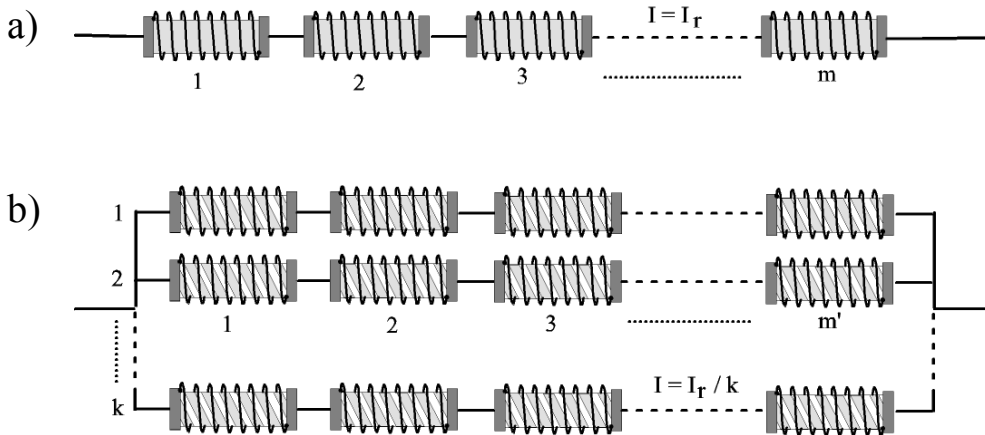


Fig 2. Arrangement of components for tube-in-coil design (a) and coil-in-coil-design (b), schematic. The total number of needed components remains roughly the same, see text.

The superconducting coils of CULT 110 are based on MCP BSCCO 2212 tubes with an outer diameter of 50 mm, the same as used in CURL 10. Superconducting ceramic tubes can be cut to mono- (see Figure 1) or bifilar coils by milling or sawing [8]. For CULT 110 a monofilar design is preferred instead of the bifilar coils used in CURL 10, because of high voltage issues. Indeed, in the case of lightning surges a high voltage wave front propagates along the conductor and in the case of bifilar coils huge voltages may appear between the first turns of the coil.

The wall thickness of the coils has to be chosen as small as possible in order to minimise the AC losses. Also, due to self-field effects, the critical current density decreases with increasing wall thickness. However, mechanical stability has to be ensured and the total number of components has to be limited. Trade-off suggests the wall thickness of 2 mm.

The needed total superconducting cross section A_{SC} is given by the specified operating current I_r and the assumption that the AC maxima of the rated current must just remain below the critical current of the component. With $j_c(77K) = 1450 \text{ A/cm}^2$ we obtain a total cross section of:

$$A_{SC} = I_r \cdot \sqrt{2} / j_c = 1.8 \text{ cm}^2 \quad (1)$$

With $k = 10$ components connected in parallel, a wall thickness of 2 mm and a cutting width of 1.5 mm a pitch of 10.5 mm results.

The minimum superconducting length is defined by the temperature T_{\max} acceptable during a short circuit. The corresponding maximum electric field E_{\max} is evaluated in an adiabatic approximation:

$$\frac{E_{\max}^2}{\rho_{SC}} \cdot t_{\text{lim}} = \int_{T_{LN}}^{T_{\max}} C_{SC}(T) dT \quad (2)$$

where ρ_{SC} is the mean resistivity in the relevant temperature range and $C_{SC}(T)$ the well-known temperature-dependent specific heat per volume. With $T_{\max} = 300 \text{ K}$ we obtain $E_{\max} = 320 \text{ V/m}$. Assuming a double line-to-ground fault (i.e. the worst case), the minimum required superconducting length is 231 m. With an active tube-length of 260 mm and a winding pitch of 10.5 mm, a superconducting length of 360 cm per component results. This leads to the total number of 650 components per phase.

III. TRIGGER COIL DESIGN

The geometry of the parallel coil is of crucial importance. The radius of the coil r has to be as small as possible in order to minimise the inductance and the time constant $\tau = L/R \sim r$. For similar reason the coil has to be as short as possible, but with the superconducting windings positioned entirely in the homogeneous field region. Three parameters then remain to be chosen independently: The material, i.e., the specific resistance $\rho_{Tr}(T)$, the number of windings N_{Tr} and the cross section A_{Tr} of the conductor. However, there are three physical arguments which restrict the possible coil configurations:

(1) Current limitation

The sum of both currents, through the shunt coil I_{shunt} and through the superconductor I_{SC} , must remain below the specified limited current I_k . The I_{SC} is calculated from the geometry of the superconductor and its resistivity $\rho_{\text{SC}}(T)$, the impedance Z of the trigger coil is obtained with the usual approximations for a long coil:

$$Z^2 = R^2 + (\omega L)^2 = \left(\frac{\rho_{\text{Tr}} \cdot 2\pi r \cdot N_{\text{Tr}}}{A_{\text{Tr}}} \right)^2 + \left(\frac{\omega \cdot \mu_0 \cdot N_{\text{Tr}}^2 \cdot \pi r^2}{l_{\text{Tr}}} \right)^2 \quad (3)$$

A numerical evaluation including the phase shift and the coupling between both inductances then allows one to calculate the maximum possible cross section A_{Tr} as function of the number of turns N_{Tr} .

(2) Heating of the coil

The heating of the trigger coil during quench must be limited. It is essentially given by the resistivity of the material $\rho_{\text{Tr}}(T)$. If a temperature increase ΔT is accepted, the condition

$$\int_0^{t_{\text{lim}}} P(t) dt \leq \int_{T_{\text{LN}}}^{T_{\text{LN}} + \Delta T} C_{\text{Tr}}(T) dT \quad (4)$$

must remain fulfilled. Here, $P(t)$ is the electric power dissipated within the trigger coil, $C_{\text{Tr}}(T)$ the temperature dependent heat capacity of the coil and T_{LN} the temperature of the coolant. In a rough approximation (4) simply defines the minimum length of the conductor and thus the minimum number of windings. A closer examination shows that this minimum number slightly depends on the cross section A_{Tr} , because of the inductive part in (3).

(3) Geometric limitations

A single layer coil is strongly preferred because of high voltage issues. Also, due to large electromechanical forces in the limiting case, for mechanical stability reasons the coil spiral is preferably cut from a metal tube. The cutting procedure defines the upper limit for thickness. Obviously, with increasing number of turns the possible cross section decreases.

For each conceivable material, a numerical study including the temperature dependences of ρ_{Tr} and C_{Tr} , visualises these three conditions by three lines in the A_{Tr} versus N_{Tr} diagram shown in Figure 3. These lines limit an area in the $(A_{\text{Tr}}, N_{\text{Tr}})$ space which reflects possible configurations in accord with specifications and physical restrictions. Figure 3 shows the $(A_{\text{Tr}}, N_{\text{Tr}})$ plots for copper (Figure 3a) and stainless steel (Figure 3b).

Two additional physical arguments are helpful: The trigger field has to be large and has to increase as rapidly as possible. For a qualitative consideration of both requirements, we assume a step-type increase U_{Step} of voltage ('hot spot')

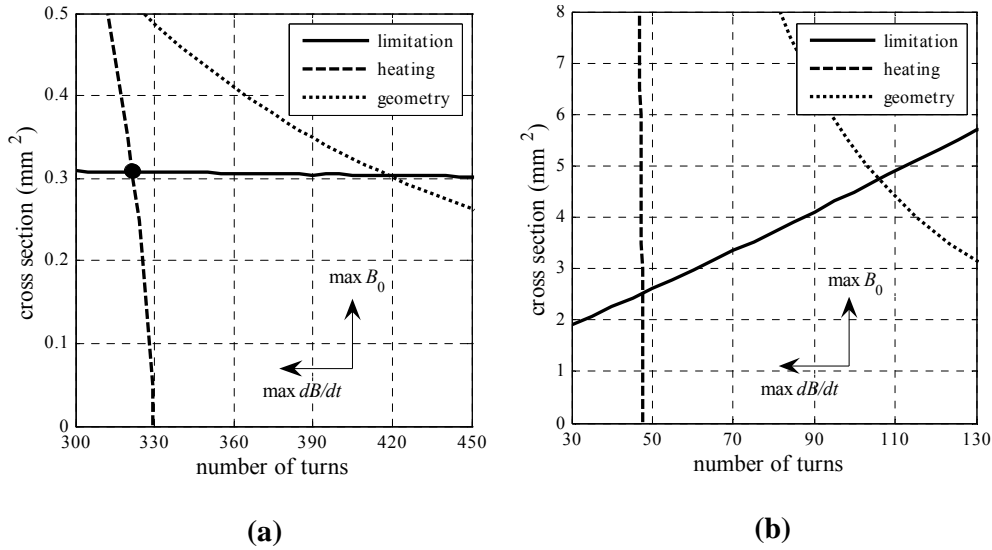


Fig 3. Winding/cross-section diagrams for copper (a) and stainless steel (b). Only trigger coils within the surface delimited by the three lines and by the N_{Tr} -axis are allowed according to physical restrictions (see text).

and consider the response of the current: $I(t) = I_0 \cdot (1 - \exp(-t/\tau))$ with $I_0 = U_{Step} / R$ and $\tau = L / R$. The initial rate of field increase is then

$$\frac{dB}{dt}(t=0) = \mu_0 \cdot \frac{N_{Tr}}{l} \cdot \frac{dI}{dt} = \mu_0 \cdot \frac{N_{Tr}}{l} \cdot \frac{I_0}{\tau} = \mu_0 \cdot \frac{N_{Tr}}{l} \cdot \frac{U_{Step}}{L} = \frac{U_{Step}}{N_{Tr} \cdot \pi r^2} \quad (5)$$

This rate increases with decreasing N_{Tr} , independently of A_{Tr} , whereas the equilibrium field

$$B_0 = \frac{\mu_0 \cdot N_{Tr} \cdot U_{Step}}{l \cdot R} = \frac{\mu_0 \cdot N_{Tr} \cdot U_{Step} \cdot A_{Tr}}{l \cdot \rho_{Tr}(77K) \cdot N_{Tr} \cdot 2\pi r} = \frac{\mu_0 \cdot U_{Step} \cdot A_{Tr}}{l \cdot \rho_{Tr}(77K) \cdot 2\pi r} \quad (6)$$

increases with increasing A_{Tr} , independently of N_{Tr} . Consequently, for the target coil N_{Tr} must be as small as possible, and A_{Tr} as large as possible (qualitatively depicted by the arrows in Figure 3).

In the case of copper shown in Figure 3(a), these rules lead to a straightforward design, *i.e.*, the coil has to be chosen corresponding to the left crossing point in Figure 3(a) marked by the full dot. However for other materials such as brass or stainless steel, the latter shown in Figure 3(b), the decision is less evident because the line defined by limitation strongly increases with N_{Tr} and a compromise between both requirements (5) and (6) has to be found.

VI. NUMERICAL SIMULATION

The final optimisation of the target coil with respect to quench homogenisation, in particular the choice of the material and, where required, the exact position on the line given by current limitation, *e.g.*, as in Figure 3(b), can be done by experiment or simulation. To this purpose a numerical tool was developed within MATLAB. The electric properties of both coils, including their cross-correlation, follow directly from their geometry. The $U(I)$ -characteristics of the superconductor were measured as functions of field and temperature [7] and parameterised with simple analytic expressions. The temperature-dependent specific heat and resistivity are well known. Heat conduction was neglected, since within the short limitation time of 60 ms the process is adiabatic. The central point of the model is the introduction of a well-defined hot spot. A simple way to do this is to assume a reduction of cross section (bubble, small crack), in our case by 3 %. The length of the hot spot (*e.g.* 1 mm) is not critical for the simulations if it is negligible compared to the total length of the superconductor. A similar simulation model has already been described in detail [6].

The simulation depicted in Figure 4 dramatically demonstrates the beneficial effect of the magnetic field. The copper coil of Figure 3(a) (full dot) was chosen for this simulation. The prospective fault current was only 6 times the rated current, a range particularly dangerous with respect to quench inhomogeneity. Prospective and limited current are depicted, as well as the temperatures of the hot spot and of the remaining of the superconductor. Figure 4(a) shows the results of the simulation described above, Figure 4(b) shows the same results, but with the influence of the magnetic field switched numerically to zero, *i.e.*, the coil acts only

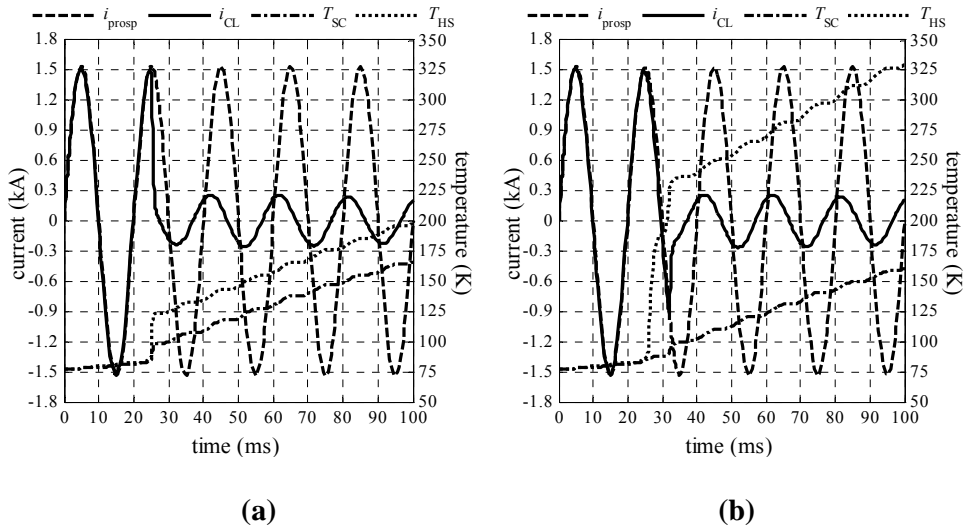


Fig 4. Simulated limitation behaviour of a superconducting component with a weak segment (hot spot). Prospective fault current (i_{prosp} , dashed line) and limited current (i_{CL} , full line) are depicted as well as the temperature of the superconductor (T_{SC} , dash-dots) and of the weak segment (T_{HS} , dots); (a) with magnetic field acting, (b) without magnetic field (see text)

as an electrical bypass.

The influence of the magnetic field on quench homogenisation is obvious. The transition of the bulk happens one half wave earlier, and the temperature of the hot spot is strongly reduced. This results in a reduction of the temperature difference between hot spot and the remaining of the bulk (from more than 150K to about 30 K) and clearly contributes to protection of the component.

Indeed, the minimisation of hot spot temperature is the objective of the simulation with different coils. For each material (copper, brass, stainless steel, aluminium) the coil was optimised with respect to its position in the (A_{Tr}, N_{Tr}) diagram. Subsequently, the corresponding coils were compared. The copper coil of cross-section and number of turns marked by the full dot in Figure 3(a) gave rise to the lowest temperature of the hot spot and will therefore be used in the CULT 110 demonstrator.

V. SHORT CIRCUIT EXPERIMENTS

Short circuit tests with the tube-in-coil geometry were already successful [7]. In the following, first limitation experiments with coil-in-coil geometry are presented. Unfortunately, in these experiments still a suboptimal stainless steel coil was used. Its performance with respect to quench homogenisation is expected to be somewhat weaker compared to the copper coil (full dot in Figure 3(a)). Also, the lengths of the superconducting coil and of the bypass coil are scaled down by a factor of 2/3 due to experimental restrictions. This assembly was tested in 67 short circuits each lasting 60 ms. Between and after these experiments no degradation of the superconductor was observed.

In the short circuit experiment shown in Figure 5 the prospective peak current of 10.2 kA (full load) is limited to less than 3.7 kA within the first half wave and further to 1.1 kA_{rms} at the specified limit. The voltage during limitation corresponds to the design field of 3.2 V_{rms}/cm.

VI. CONCLUSION

In order to reduce the normal losses of the system the component design of CULT 110 has been improved considerably by extending the self-triggered magnetic homogenisation concept to a coil-in-coil geometry. Numerical simulation and first experiments clearly show that the concept is viable and that the protection mechanism works. This has been also confirmed with partial loads and in parallel operation, however not yet with the desired reproducibility. The next steps are the use of optimum trigger coils and a pre-prototype test with several components connected in parallel and in series.

ACKNOWLEDGEMENTS

The authors want to thank A. Kudymow, S. Bemert and R. Dommerque for valuable contributions, and the BMBF/VDI for support by Grant 13N8868.

REFERENCES

- [1] M. Noe and M. Steurer, *Supercond. Sci. Technol.*, **20**, R15 (2007)
- [2] M. Chen, W. Paul, M. Lakner, L. Donzel, M. Hoidis, P. Unternaehrer, R. Weder, M. Mendik, *Physica C*, **372–376**, 1657.(2002)
- [3] J. Bock, F. Breuer, H. Walter, S. Elschner, M. Kleimaier, R. Kreutz, M. Noe, *IEEE Trans. Appl. Supercond.*, **15**, 1955 (2005).
- [4] X. Yuan, K. Tekletsadik, L. Kovalsky, J. Bock, F. Breuer, S. Elschner, *IEEE Transact. Appl. Supercond.*, **15**, 1982 (2005).
- [5] A. Usoskin, H.C. Freyhardt, A. Issaev, J. Knoke, J. Dzick, M. Collet, P. Kirchesch, J. Lehtonen, *IEEE Transact. Appl. Supercond.*, **13**, 1972 (2003).
- [6] M. Stemmler, C. Neumann, F. Merschel, U. Schwing, K.H. Weck, M. Noe, F. Breuer and S. Elschner, *IEEE Transact Appl. Supercond.*, **17**, 2347 (2007).
- [7] S. Elschner, F. Breuer, H. Walter, M. Stemmler, J. Bock, *IEEE Transact. Appl. Supercond.*, **17**, 1772 (2007).
- [8] S. Elschner, F. Breuer, M. Noe, T. Rettelbach, H. Walter, J. Bock, *IEEE Trans. Appl. Supercond.*, **13**, 1980 (2003).